DEKKER REPRINT PROGRAM

Evapotranspiration, Remote Sensing of

W. P. Kustas
United States Department of Agriculture (USDA), Beltsville, Maryland, U.S.A.

G. R. Diak
University of Wisconsin, Madison, Wisconsin, U.S.A.

M. S. Moran
United States Department of Agriculture (USDA), Tucson, Arizona, U.S.A.

INTRODUCTION

For over two decades, approaches to sense evapotranspiration (ET) remotely have made use of radiometric surface temperatures [$T_R(\theta)$, where θ is the radiometer viewing angle] as a key surface boundary condition in the land–surface energy balance. Such methods include simple flux–profile (single-level) models of surface exchange, statistical/analytical schemes, and other techniques that are based on more complex physical models of the land surface, including the so-called soil–vegetation–atmosphere–transfer (SVAT) schemes.[1]

Typically, these methods estimate fluxes through the evaluation of a surface–air temperature gradient at a single time. The aerodynamic resistance to heat transfer is largely defined by the aerodynamic roughness length, and the land surface is treated as a single effective surface in contact with the atmosphere. Any factor that introduces errors into the evaluation of this gradient, as well as the simplifications of the model, may introduce significant errors in the resulting flux estimates.

This article gives a brief overview of some of the modeling schemes that have utilized remotely sensed surface temperature data. Some recent modeling efforts will be described that address the limitations described below. These include 1) uncertainty in T_R (θ); 2) observations of T_A at regional scales; and 3) non uniqueness of the radiometric–aerodynamic temperature relationship. The resulting modeling framework leads to a more reliable scheme for quantifying ET at regional scales using satellite remote sensing.

SOURCES OF ERROR IN ET ESTIMATION

Even after performing the corrections for atmospheric attenuation and surface emissivity required to obtain a radiometric surface temperature from a satellite-measured brightness temperature, there remains 1–3° uncertainty in $T_R(\theta)$. Compounding this is the fact that vegetation density, architecture, and angle of view of the radiometer also have significant effects on brightness temperature observations (the angle-of-view "effect" being most pronounced for surfaces with partial canopy cover). As a result of these error sources, estimates of the surface–air temperature gradient and resulting fluxes are likely to have large uncertainties.[2]

An additional complication is the significant differences that exist between the radiative and the so-called "aerodynamic" (single level, "effective") surface temperature.[3] Unfortunately, this aerodynamic temperature is a construct that cannot be measured and many of the factors affecting the radiometric temperature are not well correlated to the aerodynamic roughness, making radiometric–aerodynamic temperature relationships somewhat ambiguous to begin with.

For applications over regional scales, deriving the required meteorological upper boundary conditions [i.e., shelter-or anemometer-level (2 m–10 m) air temperature and wind speed] for each satellite pixel may also lead to significant errors in flux evaluations. Typically, these meteorological quantities come from an analysis of hourly weather observations (observations typically spaced on the order of 100 km apart), and may not be representative of actual conditions at a given location.

OVERVIEW OF REMOTE SENSING METHODS

The most common way to estimate ET is to solve for the latent heat flux, LE, as a residual in the energy balance equation for the land surface:

$$LE = R_N - G - H \tag{1}$$

where R_N is the net radiation, G, the soil heat flux, and H,

the sensible heat flux all usually given in $W m^{-2}$. The quantity $R_N - G$ is commonly called the "available energy"; remote sensing methods for estimating these components are described in Kustas and Norman.[1] Typically with reliable estimates of remotely sensed solar radiation (e.g., Ref. 4), differences between remote sensing estimates and observed $R_N - G$ are within 10%.

The largest uncertainty in estimating LE comes from computing H. A simple form to express and examine the relationship between H and the surface–air temperature difference is via a resistance relationship (e.g., Ref. 5),

$$H = \rho C_P \frac{T_R(\theta) - T_A}{R_A + R_{EX}} \tag{2}$$

In this equation, T_A is the near-surface air temperature, ρ, the air density, C_P, the specific heat of air, R_A, the aerodynamic resistance and R_{EX}, the so-called "excess resistance," which addresses the fact that momentum and heat transport from the roughness elements differ.[6] The method offers the possibility of mapping surface heat fluxes on a regional scale by using radiometric temperature observations, $T_R(\theta)$ (converted from satellite brightness temperatures) if R_A and R_{EX} can be estimated appropriately. R_{EX} has been related to the ratio of roughness lengths for momentum, z_{OM}, and heat, z_{OH}, and the friction velocity u^* having the form[5,6]

$$R_{EX} = k^{-1} \ln\left(\frac{z_{OM}}{z_{OH}}\right) u^{*-1} \tag{3}$$

where $k = 0.4$ is von Karman's constant. While addressing the well-known differences in efficiency between momentum and heat transport from natural surfaces, this model is just one of several that have been developed (e.g., Refs. 5 and 7). There have been numerous efforts in recent years to apply Eq. 2 and hence determine the behavior of R_{EX} or z_{OH} for different surfaces, but no universal relation exists for land surfaces with large spatial and temporal variations in the magnitude of z_{OH} having been documented.[1] These results are due, in part, to the fact that this formulation lumps view angle dependency of $T_R(\theta)$ into the excess resistance, which makes the relation useless for any conditions except those similar to the training data.[8] Nevertheless, the method for estimating ET using the approach summarized in Eqs. 1–3 is still widely applied.

Satellite observations are essentially "instantaneous" or merely "snap shots" of the surface conditions. For many practical applications, LE estimates over longer time scales (daily values or longer) are needed. This was the impetuous for an empirical scheme for estimating daily LE, LE_D, suggested by Jackson, Reginato, and Idso[9] using observations of $T_R(\theta)$ and T_A near mid-day or maximum heating:

$$LE_D = R_{N,D} - B(T_{R,i}(\theta) - T_{A,i})^n \tag{4}$$

where the subscript i and D represent "instantaneous" and daily values, respectively. The coefficients B and n have been related to physical properties of the land surface and atmosphere, such as z_{OM} and stability, respectively.[10] Both theoretical and experimental studies have evaluated Eq. 4 lending further support for its utility as a simple technique for estimating LE_D.[11–13] In fact, studies have applied Eq. 4 to meteorological satellites for longer term regional ET monitoring.[14]

A major drawback with these approaches summarized above, however, is that there is no distinction made between soil and vegetation canopy contributions to land-surface fluxes or to satellite-measured brightness temperatures used to diagnose the fluxes. Hence, vegetation water use or stress cannot be evaluated. Furthermore, as evidence from many previous studies both the resistances in Eq. 2 and consequently the B parameter in Eq. 4 are not uniquely defined by surface roughness parameters. In addition to experimental evidence (e.g., Refs. 15 and 16), Kustas et al.[8] using SVAT simulations, have shown the lack of a unique relationship between $T_R(\theta)$ and the aerodynamic surface temperature, T_O, (satisfying the flux relationship in Eq. 2 when used with traditional expressions for the resistances; see Ref. 2).

An alternative approach proposed recently considers the soil and vegetation contribution to the total or composite heat fluxes and soil and vegetation temperatures to the radiometric temperature measurements in the so-called "Two-Source" Modeling (TSM) scheme.[17] This allows for Eq. 2 to be recast into the following expression:

$$H = \rho C_P \frac{T_R(\theta) - T_A}{R_R} \tag{5}$$

where R_R is the radiometric–convective resistance given by[17]

$$R_R = \frac{T_R(\theta) - T_A}{\dfrac{T_C - T_A}{R_A} + \dfrac{T_S - T_A}{R_A + R_S}} \tag{6}$$

where T_C is the canopy temperature, T_S, the soil temperature, and R_S, the soil resistance to heat transfer. An estimate of leaf area index or fractional vegetation cover, f_C, is used to estimate T_C and T_S from $T_R(\theta)$:

$$T_R(\theta) \approx \left(f_C(\theta) T_C^4 + (1 - f_C(\theta)) T_S^4\right)^{1/4} \tag{7}$$

where $f_C(\theta)$ is the fractional vegetative cover at radiometer viewing angle θ, and R_S is computed from a relatively simple formulation predicting wind speed near the soil

surface.[17] With some additional formulations for estimating canopy transpiration, and the dual requirement of energy, and radiative balance of the soil and vegetation components, closure in the set of equations is achieved. Through model validation studies, revisions to the original two-source formulations have been made improving its utility under a wider range of the environmental conditions.[8,18]

Several relatively early studies recognized the need to assess the impact of vegetation cover on remote methods for deriving ET. For example, Price[19] used information provided in the Vegetation Index–radiometric temperature, VI–$T_R(\theta)$, space. This work involved the use of an energy balance model for computing spatially distributed fluxes from the variability within the Normalized Difference Vegetation Index, NDVI–$T_R(\theta)$ space from a single satellite scene. NDVI was used to estimate the fraction of a pixel covered by vegetation and showed how one could derive bare soil and vegetation temperatures and, with enough spatial variation in surface moisture, estimate daily ET for the limits of full cover vegetation, dry and wet bare soils.

Following Price,[19] Carlson, Gillies, and Perry[20] combined an Atmospheric Boundary Layer (ABL) model with a SVAT for mapping surface soil moisture, vegetation cover, and surface fluxes. Model simulations are run for two conditions: 100% vegetative cover with the maximum NDVI being known a priori, and with bare soil conditions knowing the minimum NDVI. Using ancillary data, including a morning atmospheric sounding, vegetation and soil type information, root-zone and surface

soil moisture are varied, respectively, until the modeled and measured $T_R(\theta)$ are closely matched for both cases so that fractional vegetated cover and surface soil moisture are derived. Comparisons between modeled–derived fluxes and observations have been made recently by Gillies et al.[21] indicating approximately 90% of the variance in the fluxes was captured by the model.

In a related approach, Moran et al.[22] defined theoretical boundaries in VI–$(T_R(\theta)-T_A)$ space using the Penman–Monteith equation. The boundaries define a trapezoid, which has at the upper two corners unstressed and stressed 100% vegetated cover and at the lower two corners, wet and dry bare soil conditions (Fig. 1). In order to calculate the vertices of the trapezoid, measurements of R_N, vapor pressure, T_A, and wind speed are required as well as vegetation specific parameters; these include maximum and minimum VI for the full-cover and bare soil case, maximum leaf area index, and maximum and minimum stomatal resistance. Moran et al.[22] analyze and discuss several of the assumptions underlying the model, especially those concerning the linearity between variations in canopy–air temperature and soil–air temperatures and transpiration and evaporation. Information about ET rates are derived from the location of the VI–$[T_R(\theta)-T_A]$ measurements within the date and time-specific trapezoid. This approach permits the technique to be used for both heterogeneous and uniform areas and thus does not require having a range of NDVI and surface temperature in the scene of interest as required by Carlson, Gillies, and Perry[20] and Price.[19] Moran[23] compared the method for estimating relative rates of ET with
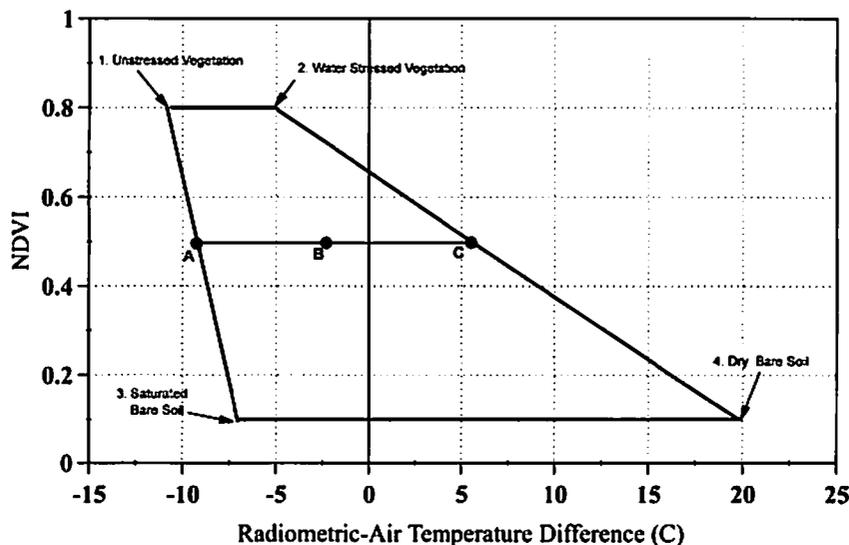

Fig. 1 The trapezoidal shape that results from the theoretical relation between radiative temperature minus air temperature [$T_R(\theta)$ − T_A] and the NDVI from Moran et al.[22] With a measurement of ($T_R(\theta)$ − T_A) at point C, it would be possible to equate the ratio of actual to potential LE with the ratio of distances CB and AB.

observations over agricultural fields and showed it could be used for irrigation scheduling purposes.

These modeling schemes, however, are vulnerable to errors in the radiometric temperature observations and most require screen level meteorological inputs (primarily wind speed, u, and air temperature, T_A, observations) which at regional scales suffer from errors of representativeness (observation not taken at the same location where flux estimates are performed). Approaches using remotely sensed data for estimating the variation of these quantities are being developed and tested.[24,25] How reliable the algorithms are for different climatic regimes needs to be evaluated.

A robust modeling framework to address some of these limitations was proposed early on in the application of satellite observations by Wetzel Atlas, and Woodward[26] Strictly speaking, the Wetzel et al. study was aimed at the estimation of soil moisture from remotely sensed data, but an evaluation of surface fluxes is implicit in the scheme. The study recognized that using a time rate of change in $T_R(\theta)$ from a geostationary satellite such as from the Geosynchronous Operational Environmental Satellite (GOES) coupled to an ABL model could mitigate some of the inherent problems arising from the use of single-time-level data, such as atmospheric corrections, emissivity, and instrument calibration. By using time rate of change of $T_R(\theta)$, one reduces the need for absolute accuracy in satellite calibration, and atmospheric and emissivity corrections, all significant challenges (see Refs. 1 and 8). Diak and Whipple[27] implemented this approach with a method for partitioning the available energy into LE and H by using the rate of rise of $T_R(\theta)$ from GOES and ABL growth and included a procedure to account for effects of horizontal and vertical temperature advection and vertical motions above the ABL.

Further refinements to these time-rate-of-change schemes have been recently developed[28,29] that use an energy closure scheme based on energy conservation within the ABL. The so-called Atmospheric–LandEXchange-Inverse (ALEXI) model uses a simple slab model of the time-development of the ABL in response to heat input to the lower atmosphere. A profile of atmospheric temperature at the initial time (usually from an analysis of synoptic data) serves as the upper boundary condition in atmospheric temperature. Through surface–ABL energy balance considerations and implementation of the TSM scheme for the land surface component of the model,[17] ALEXI couples ABL development to the temporal changes in surface radiometric temperature from GOES and fraction vegetation cover from Advanced Very High Resolution Radiometer, AVHRR–NDVI. The advantages of using temporal changes in brightness temperature measurements have been noted. With an energy balance method utilizing the temporal change of ABL structure, errors that arise in

schemes utilizing shelter-level (~ 2 m above ground level) measurements of air temperature (to estimate the surface–air temperature gradient) for estimating the heat fluxes are also mitigated. Approaches that utilize this surface–air temperature gradient, typically evaluated within 10 m of the surface, are very sensitive to errors in the evaluation of the gradient arising from errors both in the representativeness of the air temperature measurements, and errors in evaluating radiometric temperatures.

Another much simpler scheme, which also uses the TSM framework, employs the time rate of change in radiometric temperature and air temperature observations from a nearby weather station in a simple formulation for computing regional heat fluxes, called the Dual-Temperature-Difference (DTD) approach.[30] Although this technique requires air temperature observations, by using a time difference in air temperature, errors caused by using local shelter level observations for representing a region are still reduced. Moreover, the scheme is simple, thus it is computationally efficient and does not require atmospheric sounding data for initialization.

APPLICATION OF ALEXI AND DTD METHODS

An example of the utility of the DTD approach is presented at the field scale using ground-based $T_R(\theta)$ observations and regional weather station data from sites in subhumid and semiarid climatic regions (i.e., Oklahoma and Arizona). In addition, a comparison of regional scale heat fluxes between the more rigorous ALEXI model and the simple DTD method using satellite data over the U.S. Great Plains is presented.

With the field scale $T_R(\theta)$ observations, the comparisons in Fig. 2 are LE estimates using the original TSM approach and the DTD scheme with regional weather station data (T_A and u) collected 50 km–100 km away from the site compared to on-site flux tower observations.[30] There is considerably more scatter using the TSM vs. the DTD approach with nonlocal meteorological inputs resulting in a Root Mean Square Error (RMSE) on the order of 100 W m^{-2}. Using the DTD scheme, there is a significant reduction in scatter with the flux observations yielding almost a 40% reduction in error with a RMSE $\sim 65 \text{ W m}^{-2}$.

To illustrate a regional application of the DTD and ALEXI approaches, GOES brightness temperature data and NOAA–AVHRR satellite observations were used with surface synoptic data for July 2, 1997 over the U.S. Great Plains, same case study used by Mecikalski et al.[29]. The domain investigated was divided into 10 km × 10 km grid cells, with 223 cells east-to-west and 201 in the meridional direction, a total of 44,823 cells. NOAA–AVHRR–NDVI product for the region was utilized to estimate fractional
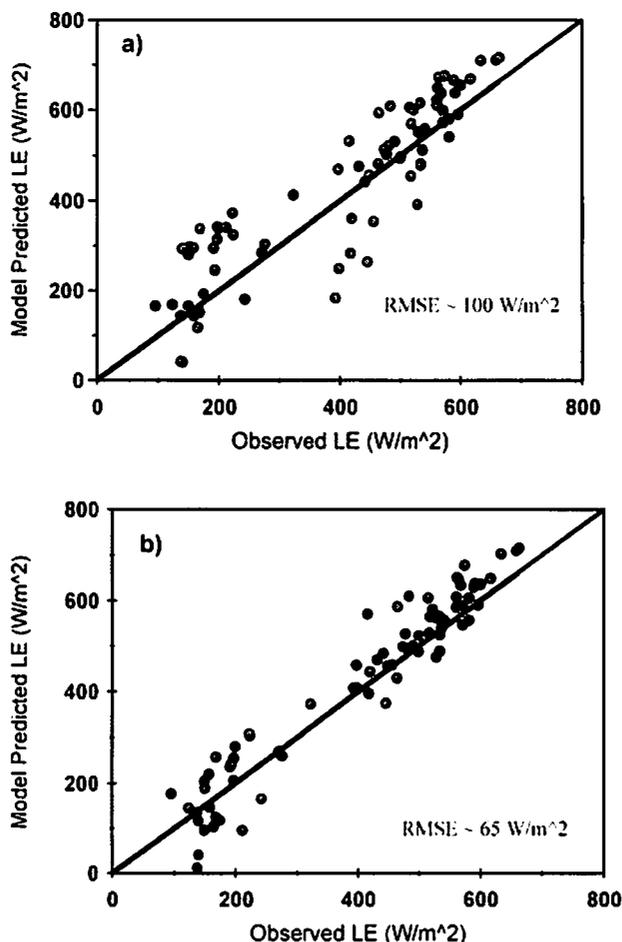
Fig. 2 Comparison between observed and modeled mid-day latent heat flux, LE, using (a) original TSM scheme and (b) DTD approach. Regional T_A and u observations are from weather stations $\sim$ 50 km to $\sim$ 100 km away from study site. Line represents perfect agreement with observations.

vegetation cover. Hourly GOES brightness temperature measurements for the region were cloud screened and subsequently linearly time-interpolated to 1.5 hr and 5.5 hr after local sunrise. These top-of-atmosphere brightness temperatures were then atmospherically corrected to estimate surface radiometric surface temperatures and corrected for emissivity using land surface classification data (for details, see Ref. 29).

The estimates of LE for 5.5 hr after local sunrise for the domain are shown in Fig. 3 from the DTD and ALEXI schemes. Areas that are white in this figure were either those identified as cloudy by screening procedures, and thus were not evaluated in either method, or did not achieve model convergence (primarily ALEXI). The DTD method displays very similar spatial features as the ALEXI output, although, as shown, there is a systematic difference between the two, with the DTD method showing overall higher values of LE.

Unlike ALEXI, in which air temperature is dynamically determined within the scheme, in the DTD method, air temperature is a measured (from surface synoptic data) and invariant upper boundary condition for the model. The horizontal spacing of hourly synoptic air temperature measurements is roughly 100 km, while the satellite data and the DTD grid on which the $T_R(\theta)$ and NDVI data are applied have a significantly higher resolution. With fixed boundary conditions measured on the scale of 100 km, DTD cannot account for the sub-synoptic-scale interactions between surface radiometric temperatures and air temperature, as does ALEXI. Nevertheless, results from the DTD procedure are encouraging in their ability to duplicate the spatial patterns from ALEXI, a much more complicated and data-intensive parameterization. Computer processing time for the domain shown in Fig. 3 for the ALEXI model was
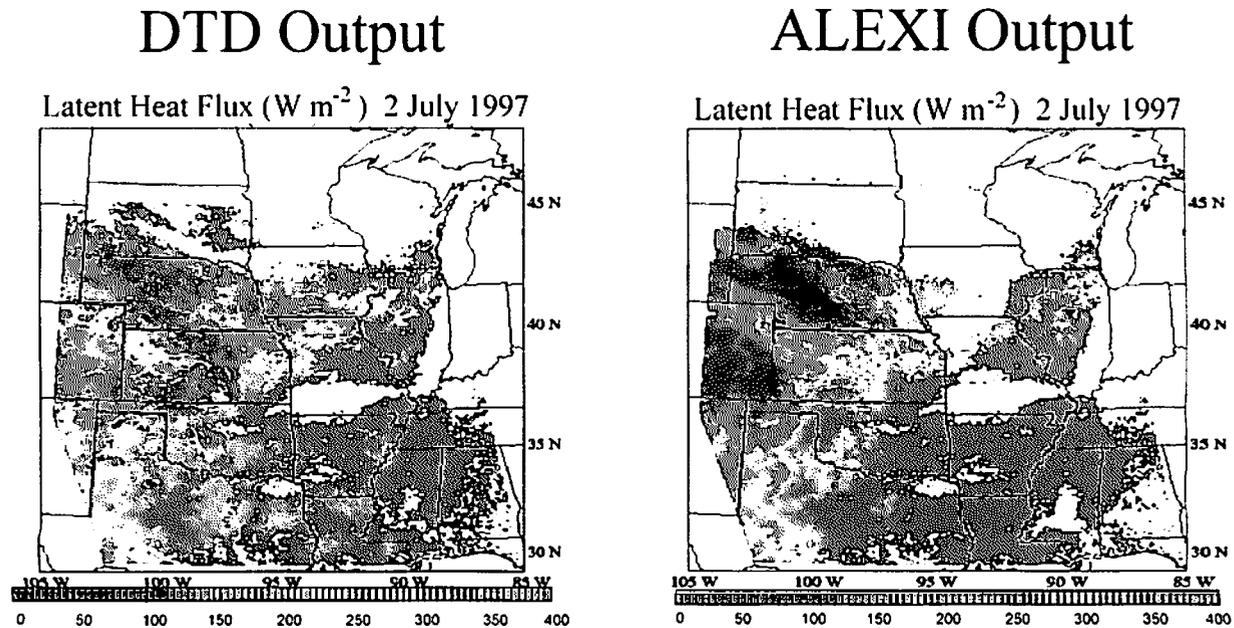
DTD Output

Latent Heat Flux (W m^{-2}) 2 July 1997

ALEXI Output

Latent Heat Flux (W m^{-2}) 2 July 1997

Fig. 3 Regional scale latent heat flux maps from DTD and ALEXI ~5.5 hr after local sun rise for the U.S. Great Plains region on July 2, 1997.

about 35 min, while the DTD scheme required less than 1 min of processing time on the same UNIX workstation.

CONCLUSION

Current efforts incorporating remote sensing data into SVAT modeling schemes that accommodate the fundamental differences between aerodynamic and radiometric temperatures and that are not sensitive to measurement errors should greatly enhance the prospect of quantifying ET at regional scales with remote sensing. The measurement errors with the largest impact on ET estimation are atmospheric and emissivity effects in converting satellite brightness temperatures to radiometric surface temperatures and assigning meteorological variables, primarily air temperature, for each satellite pixel from regional weather station observations.[28] Due to limited spatial observations of atmospheric properties, the uncertainty in the surface–air temperature difference is likely to be several degrees resulting in unreliable ET estimation, which have significantly hampered many past modeling approaches.

Although the current approaches described here, ALEXI and DTD, address most of these limitations, there is a drawback to these schemes in that the source of radiometric temperatures (GOES), and the atmospheric boundary layer closure and weather station network

dictate an output resolution of 5 km–10 km. For many applications, particularly evaluating ET for individual fields, these 5 km–10 km estimates are at a much coarser spatial scale. Unfortunately, temporal changes (1/2-hourly) of satellite brightness temperatures are only available from GOES at a minimum resolution of ~5 km. Other satellites have much finer spatial resolution, such as the Land Remote-Sensing Satellite (Landsat) and the Advanced Spaceborne Thermal Emission Reflectance Radiometer (ASTER), but have much coarser temporal coverage (~16 days).

Kustas and Norman[31] found subpixel variability in surface properties can result in large errors in pixel-average heat flux estimation, using pixel-average inputs when there is a significant discontinuity in surface conditions, particularly under low winds. A solution to the problem of spatial resolution was introduced by Norman et al.,[32] who developed a scheme for "disaggregating" ALEXI 5 km flux estimates (called DisALEXI) to the 30 m scale using high-resolution NDVI and $T_R(\theta)$ data, and the local 50 m air temperature estimate provided by ALEXI as the important atmospheric boundary condition in temperature. Although, this scheme makes use of energy conservation principles applied to ABL dynamics to deduce air temperature via ALEXI, it still does not consider local variability in mean air properties. However, the preliminary results are encouraging, suggesting disaggregation of coarse spatial resol-

ution ET output may be feasible periodically with high resolution data from Landsat or ASTER.

REFERENCES

1. Kustas, W.P.; Norman, J.M. Use of Remote Sensing for Evapotranspiration Monitoring Over Land Surfaces. Hydrol. Sci. J. des Sci. Hydrologiques 1996, 41, 495–516.
2. Hall, F.G.; Huemmrich, K.F.; Geotz, S.J.; Sellers, P.J.; Nickerson, J.E. Satellite Remote Sensing of Surface Energy Balance: Success, Failures and Unresolved Issues in FIFE. J. Geophys. Res. 1992, 97 (D17), 19061–19090.
3. Norman, J.M.; Becker, F. Terminology in Thermal Infrared Remote Sensing of Natural Surfaces. Remote Sens. Rev. 1995, 12, 159–173.
4. Diak, G.R.; Bland, W.L.; Mecikalski, J.R. A Note on First Estimates of Surface Insolation from GOES8 Visible Satellite Data. Agric. Forest Meteorol. 1996, 82, 219–226.
5. Garratt, J.R.; Hicks, B.B. Momentum, Heat and Water Vapour Transfer to and from Natural and Surfaces. Quart. J. R. Meteorol. Soc. 1973, 99, 680–687.
6. Brutsaert, W. Evaporation into the Atmosphere; D. Reidel: Dordrecht, 1982; 299 pp.
7. McNaughton, K.G.; Van den Hurk, B.J.J.M. A 'Lagrangian' Revision of the Resistors in the Two-Layer Model for Calculating the Energy Budget of a Plant Canopy. Boundary-Layer Meteorol. 1995, 74, 262–288.
8. Kustas, W.P.; Norman, J.M.; Schmugge, T.J.; Anderson, M.C. Mapping Surface Energy Fluxes with Radiometric Temperature. In Thermal Remote Sensing in Land Surface Processes; Quattrochi, D.A., Luvall, J.C., Eds.; Taylor and Francis: London, UK., 2002.
9. Jackson, R.D.; Reginato, R.J.; Idso, S.B. Wheat Canopy Temperature: A Practical Tool for Evaluating Water Requirements. Water Resour. Res. 1977, 13, 651–656.
10. Seguin, B.; Itier, B. Using Midday Surface Temperature to Estimate Daily Evaporation from Satellite Thermal IR Data. Int. J. Remote Sens. 1983, 4, 371–383.
11. Carlson, T.N.; Buffum, M.J. On Estimating Total Daily Evapotranspiration from Remote Surface Measurements. Remote Sens. Environ. 1989, 29, 197–207.
12. Lagouarde, J.-P. Use of NOAA AVHRR Data Combined with an Agrometeorological Model for Evaporation Mapping. Int. J. Remote Sens. 1991, 12, 1853–1864.
13. Carlson, T.N.; Capehart, W.J.; Gillies, R.R. A New Look at the Simplified Method for Remote Sensing of Daily Evapotranspiration. Remote Sens. Environ. 1995, 54, 161–167.
14. Seguin, B.; Lagouarde, J. P.; Saranc, M. The Assessment of Regional Crop Water Conditions from Meteorological Satellite Thermal Infrared Data. Remote Sens. Environ. 1991, 35, 141–148.
15. Vining, R.C.; Blad, B.L. Estimation of Sensible Heat Flux from Remotely Sensed Canopy Temperatures. J. Geophys. Res. 1992, 97 (D17), 18951–18954.
16. Verhoef, A.; De Bruin, H.A.R.; Van den Hurk, B.J.J.M. Some Practical Notes on the Parameter kB^{-1} for Sparse Vegetation. J. Appl. Meteorol. 1997, 36, 560–572.
17. Norman, J.M.; Kustas, W.P.; Humes, K.S. A Two-Source Approach for Estimating Soil and Vegetation Energy Fluxes from Observations of Directional Radiometric Surface Temperature. Agric. Forest Meteorol. 1995, 77, 263–293.
18. Kustas, W.P.; Norman, J.M. Evaluation of Soil and Vegetation Heat Flux Predictions Using a Simple Two-Source Model with Radiometric Temperatures for Partial Canopy Cover. Agric. Forest Meteorol. 1999, 94, 13–29.
19. Price, J.C. Using Spatial Context in Satellite Data to Infer Regional Scale Evapotranspiration. IEEE Trans. Geosci. Remote Sens. 1990, GE-28, 940–948.
20. Carlson, T.N.; Gillies, R.R.; Perry, E.M. A Method to Make Use of Thermal Infrared Temperature and NDVI Measurements to Infer Soil Water Content and Fractional Vegetation Cover. Remote Sens. Rev. 1994, 52, 45–59.
21. Gillies, R.R.; Carlson, T.N.; Cui, J.; Kustas, W.P.; Humes, K.S. Verification of the 'Triangle' Method for Obtaining Surface Soil Water Content and Energy Fluxes from Remote Measurements of Normalized Difference Vegetation Index (NDVI) and Surface Radiant Temperature. Int. J. Remote Sens. 1997, 18, 3145–3166.
22. Moran, M.S.; Clarke, T.R.; Inoue, Y.; Vidal, A. Estimating Crop Water Deficit Using the Relation Between Surface–Air Temperature and Spectral Vegetation Index. Remote Sens. Environ. 1994, 49, 246–263.
23. Moran, M.S. Irrigation Management in Arizona Using Satellites and Airplanes. Irrig. Sci. 1994, 15, 35–44.
24. Bastiaanssen, W.G.M.; Feddes, R.A.; Holtslag, A.A.M. A Remote Sensing Surface Energy Balance Algorithm for Land (SEBAL) Part 1: Formulation. J. Hydrol. 1998, 212–213, 200–213.
25. Gao, W.; Coultier, R.L.; Lesht, B.M.; Qui, J.; Wesely, M.L. Estimating Clear-Sky Regional Surface Fluxes in the Southern Great Plains Atmospheric Radiation Measurement Site with Ground Measurements and Satellite Observations. J. Appl. Meteorol. 1998, 37, 5–22.
26. Wetzel, P.J.; Atlas, D.; Woodward, R. Determining Soil Moisture from Geosynchronous Satellite Infrared Data: A Feasibility Study. J. Climatol. Appl. Meteorol. 1984, 23, 375–391.
27. Diak, G.R.; Whipple, M.A. Improvements to Models and Methods for Evaluating the Land-Surface Energy Balance and "Effective" Roughness Using Radiosonde Reports and Satellite-Measured "Skin" Temperatures. Agric. Forest Meteorol. 1993, 63, 189–218.
28. Anderson, M.C.; Norman, J.M.; Diak, G.R.; Kustas, W.P.; Mecikalski, J.R. A Two-Source Time-Integrated Model for Estimating Surface Fluxes from Thermal Infrared Satellite Observations. Rem. Sens. Environ. 1997, 60, 195–216.
29. Mecikalski, J.R.; Diak, G.R.; Anderson, M.C.; Norman, J.M. Estimating Fluxes on Continental Scales Using

E

Remotelysensed Data in an Atmosphericland Exchange Model. J. Appl. Meteorol. **1999**, *38*, 1352–1369.

30. Norman, J.M.; Kustas, W.P.; Prueger, J.H.; Diak, G.R. Surface Flux Estimation Using Radiometric Temperature: A Dual Temperature Difference Method to Minimize Measurement Error. Water Resour. Res. **2000a**, *36*, 2263–2274.

31. Kustas, W.P.; Norman, J.M. Evaluating the Effects of Sub-pixel Heterogeneity on Pixel Average Fluxes. Remote Sens. Environ. **2000**, *74*, 327–342.

32. Norman, J.M.; Daniel, L.C.; Diak, G.R.; Twine, T.E.; Kustas, W.P.; French, A.N.; Schmugge, T.J. Satellite Estimates of Evapotranspiration on the 100-m Pixel Scale. IEEE IGARRS 2000 Proc. **2000b**, IV,1483–1485.